ATP Hydrolysis Analysis of Severe Acute Respiratory Syndrome (SARS) Coronavirus Helicase

Na-Ra Lee,[†,a] A-Ram Lee,[†,a] Bokhui Lee,[‡] Dong-Eun Kim,[‡,*] and Yong-Joo Jeong[†,*]

[†]*Department of Bio and Nanochemistry, Kookmin University, Seoul 136-702, Korea. *E-mail: jeongyj@kookmin.ac.kr*
[‡]*Department of Bioscience and Biotechnology, Konkuk University, Seoul 143-701, Korea. *E-mail: kimde@konkuk.ac.kr*
Received May 15, 2009, Accepted June 11, 2009

Severe acute respiratory syndrome coronavirus (SARS-CoV) helicase separates the double-stranded nucleic acids using the energy from ATP hydrolysis. We have measured ATPase activity of SARS-CoV helicase in the presence of various types of nucleic acids. Steady state ATPase analysis showed that poly(U) has two-times higher turnover number than poly(C) with lower Michaelis constant. When M13 single-stranded DNA is used as substrate, the Michaelis constant was about twenty-times lower than poly(U), whereas turnover numbers were similar. However, stimulation of ATPase activity was not observed in the presence of double-stranded DNA. pH dependent profiles of ATP hydrolysis with the helicase showed that the optimal ATPase activities were in a range of pH 6.2 ~ 6.6. In addition, ATP hydrolysis activity assays performed in the presence of various divalent cations exhibited that Mg^{2+} stimulated the ATPase activity with the highest rate and Mn^{2+} with about 40% rate as compared to the Mg^{2+}.

Key Words: Severe acute respiratory syndrome coronavirus helicase, ATP hydrolysis, Single-stranded nucleic acids, pH-Dependence profile, Divalent cations

Introduction

Helicases are molecular motor proteins that translocate on nucleic acid (NA) and separate the double-stranded (ds) NA into two single-stranded (ss) NAs using the energy generated from nucleoside triphosphate (NTP) hydrolysis.[1-3] The strand separation activity of helicase is required for various processes of genome replication and recombination. It has been reported that defects in helicases lead to many human diseases including Bloom's syndrome, Werner's syndrome, and Xeroderma pigmentosum.[4-6] Because of importance of helicases in biological function, a lot of studies are currently being undertaken to better understand the mechanism.

The worldwide outbreak of Severe Acute Respiratory Syndrome (SARS) was caused by a novel coronavirus (CoV) and was claimed almost 800 deaths according to World Health Organization (WHO). SARS-CoV is an enveloped and has a single-stranded RNA genome of 29.7 kb.[7,8] Two large polyproteins (pp1a and pp1ab) are produced from the replicase region and these polyproteins are subsequently cleaved into individual functional polypeptides by virus-encoded main proteinase (M^{pro}).[9] This autoproteolysis leads to release of several non-structural proteins, including RNA-dependent RNA polymerase and NTPase/helicase. It has been reported that these proteins are essential for viral replication and are regarded as good targets for antiviral therapy.[10-12] Recently, helicase is an emerging novel target for the development of anti-SARS agent [13-15] and a lot of efforts have been made to find out inhibitors of SARS-CoV helicase and tested as drugs.[13-16] RNA and DNA aptamers against SARS-CoV helicase were also reported to have inhibitory effect for nucleic acid unwinding and ATP hydrolysis activities.[17,18] Previously, we have purified the SARS-CoV helicase homogeneously and isolated its RNA aptamers.[18] Moreover, we have shown that aryl diketoacids selectively inhibit dsDNA unwinding activity of SARS-CoV helicase and are potential inhibitors.[16] In the present study, ATP hydrolysis activities of SARS-CoV helicase were measured in the presence of various types of nucleic acids using steady state kinetic analysis. The effects of pH conditions of reaction buffer and divalent cations on the ATPase activity were also investigated to better describe the ATP hydrolysis activity of SARS-CoV helicase.

Materials and Methods

Protein, reagent, and buffer. The SARS coronavirus helicase expression vector, pHelA12, was transformed into *E.coli* Rosetta™ competent cells, over-expressed, and purified as described previously.[16,18] The protein concentration was determined by absorbance measurements at 280 nm in 8 M Urea (the extinction coefficient is 67, 160 $M^{-1}cm^{-1}$) and by Bio-Rad protein assay system (Bio-Rad) with bovine serum albumin as a standard. Both methods provided similar concentrations. Reaction buffer A was used throughout the experiments unless specified otherwise, which contained 50 mM Tris/Cl (pH 6.6) and 50 mM NaCl.

Poly(U) and Poly(C) were purchased from Amersham Biosciences and their concentrations were determined as described previously.[19,20] M13 ssDNA (M13mp18) was purified as described.[21]

Steady state ATPase assay. ATP hydrolysis assay was carried out by measuring the amount of inorganic phosphate (P_i) released from ATP. P_i was quantified by spectrophotometric method based on the complex formation with molybdate.[22] After various times of incubation, the reactions were stopped by adding color-developing solution (1 part of 10% ascorbic

[a]These two authors contributed equally to this work

acid and 6 part of 0.42% ammonium molybdate in 1 N H_2SO_4). The stopped reaction mixture was further incubated for 1 h at 37 °C and read at 820 nm. The amount of P_i released was quantified using the P_i standard curve. The molar concentration of P_i was plotted versus the time of reaction, and the steady state rate was obtained from the slope of initial reaction times.

To measure the steady state ATPase rate in the presence of various NAs, 100 nM helicase was mixed with 2 mM ATP, 5 mM $MgCl_2$, and various concentrations of poly(U), poly(C), or single-stranded (ss) circular M13 DNA in buffer A at 37 °C. To compare the steady state rate of ATP hydrolysis activity between ssDNA and dsDNA, 100 nM helicase was mixed with 2 mM ATP, 5 mM $MgCl_2$, and 3 nM M13 ssDNA or 1.2 nM pGEX-5X-1 plasmid dsDNA. Control experiment was performed same as above only in the absence of NA. The kinetic parameters k_{cat} (turnover number) and K_m (Michaelis constant) were determined from Equation 1.

$$v = [E]_0[S]\, k_{cat}/(K_m + [S]) \quad (1)$$

where v is the rate of the reaction, $[E]_0[S]$ is the maximal rate, [S] is the concentration of substrate, and K_m is the Michaelis constant.

The effect of pH on ATPase activity was studied at 37 °C in a pH range of 4.0 to 9.0. Several different buffer solutions (50 mM) of various pH were used as follows: sodium acetate (pH 4.0 ~ 5.0), MES (pH 5.5 ~ 6.2), and Tris/Cl (pH 6.5 ~ 9.0). 100 nM helicase was mixed with 2 mM ATP, 2 nM M13 ssDNA, 5 mM $MgCl_2$, and 50 mM NaCl in each different buffer condition. After various times of incubation, the reactions were quenched and the products were analyzed as above.

The dependence of ATP hydrolysis activity on the concentrations of several divalent cations was also studied at 37 °C. 100 nM helicase was mixed with 2 mM ATP, 2 nM M13 ssDNA, and various concentrations of $MgCl_2$, $MnCl_2$, $CaCl_2$, and Zinc acetate in buffer A. After various times of incubation, the reactions were quenched and the products were analyzed as above.

Results and Discussion

To estimate the rate of ATP hydrolysis in the presence of poly(U) and poly(C) RNAs, the released P_i was quantified by formation of molybdate complex. The ATPase activity of SARS-CoV helicase was shown to be enhanced by homopolynucleotides tested. Fig. 1(A) shows that the steady state ATPase rates increased in a hyperbolic manner with increasing poly(U) concentrations providing a turnover number (k_{cat}) of 68.0 ± 3.7 s^{-1} and a Michaelis constant (K_m) of 11.7 ± 2.5 nM. The effect of poly(C) concentration on the ATPase activity is shown in Fig. 1(B). The steady state rates also increased in a hyperbolic manner with increasing poly(C) concentrations providing a k_{cat} of 31.1 ± 2.3 s^{-1} and a K_m of 73.1 ± 18.1 nM. These results indicate that SARS-CoV helicase shows better ATPase activity in the presence of poly(U) than poly(C). When we compare the specificity constants (k_{cat}/K_m) of poly(U) and poly(C), k_{cat}/K_m value of poly(U) (~ 5.8 $nM^{-1}\cdot sec^{-1}$) is 15-times higher than the value of poly(C) (~ 0.4 $nM^{-1}\cdot sec^{-1}$).

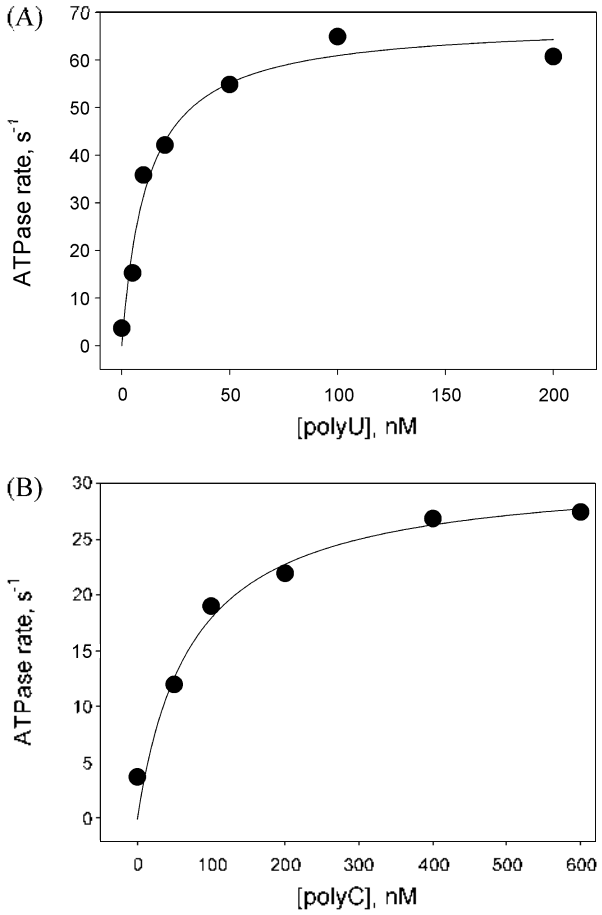

Figure 1. Measurement of ATPase activities in the presence of homopolynucleotide RNAs. 100 nM SARS-CoV helicase was mixed with 2 mM ATP, 5 mM $MgCl_2$, and various concentration of poly(U) (**A**) and poly(C) (**B**) in buffer A at 37 °C. After various times, the reactions were quenched by adding color-developing solution and released P_i was quantified using P_i standard curve. The ATPase rate *versus* [poly(U)] fit to a Equation 1 with a k_{cat} of 68.0 ± 3.7 s^{-1} and a K_m of 11.7 ± 2.5 nM. The ATPase rate *versus* [poly(C)] fit to a Equation 1 with a k_{cat} of 31.1 + 2.3 s^{-1} and a K_m of 73.1 + 18.1 nM.

This is consistent with previous report describing the ATPase activity stimulation effect was most enhanced when poly(U) was used.[23] However, it is not clear why poly(U) is better ATPase activity stimulator than other homopolynucleotide RNAs for SARS-CoV helicase.

To investigate the effect of DNA on the ATPase activity, we also carried out ATP hydrolysis analysis in the presence of M13 ssDNA. M13 ssDNA is a 7,250 bases-long circular DNA. Since it has no end, it is expected that helicase translocates along the ssDNA continuously unless the helicase separates from the DNA. Fig. 2(A) shows that the steady state ATPase rates increased in a hyperbolic manner with increasing M13 ssDNA concentrations providing a k_{cat} of 64.9 ± 1.0 s^{-1} and a K_m of 0.63 ± 0.04 nM. Interestingly, the steady state ATPase rate in the presence of 1.2 nM plasmid dsDNA (1.3 s^{-1}) is quite similar to the case performed in the absence of DNA (0.9 s^{-1}), as shown in Fig. 2(B). Unlike little stimulation of the ATPase activity with dsDNA, stimulation of ATPase activity by ssDNA is significant. Although k_{cat} value of M13 ssDNA is similar to

that of poly(U), $K_{1/2}$ value for ATP hydrolysis stimulation is much lower than that of poly(U) and poly(C). It appears that binding of SARS-CoV helicase to ssDNA is tighter than ssRNA. Other explanation would be the helicase exhibit similar preferences for nucleic acids regardless of DNA or RNA, because smaller $K_{1/2}$ value for ATP hydrolysis with the M13 ssDNA can be explained by more amounts of nucleotides (~ 7,000 nts) in one molecule than that of RNA homopolymer (100 ~ 300 nts per molecule) used in this study.

In the absence of DNA, ATP hydrolysis was negligible and about 70-times slower than the ATPase rate observed in the presence of M13 ssDNA. It is very common to almost all of helicases that nucleic acid binding stimulates the NTPase activity of helicases. Since biological role of helicase by itself is translocation along ssNA and dsNA unwinding, chemical

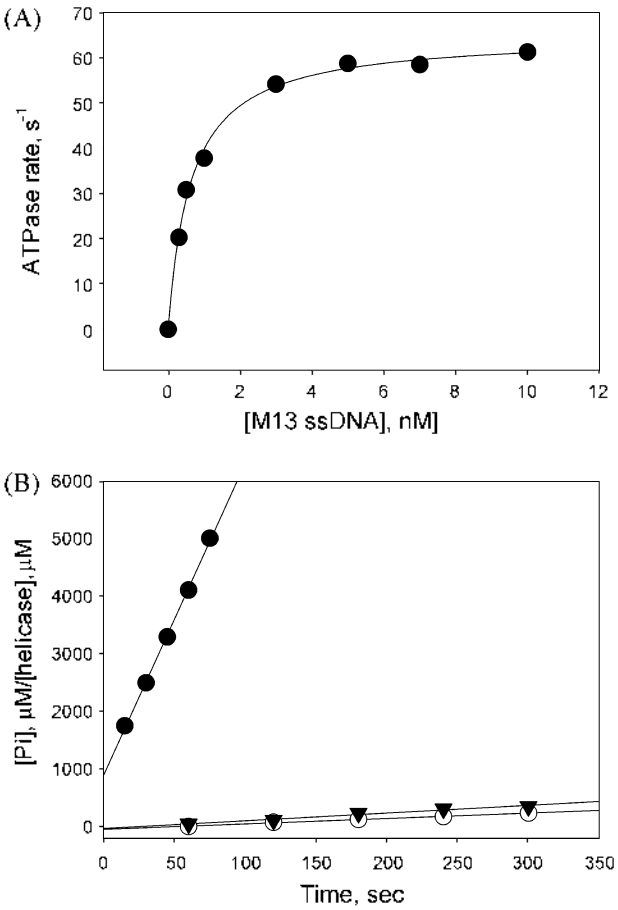

Figure 2. (A) 100 nM SARS-CoV helicase was mixed with 2 mM ATP, 5 mM $MgCl_2$, and various concentration of M13 ssDNA in buffer A at 37 °C. After various times, the reactions were quenched by adding color-developing solution and released P_i was quantified using P_i standard curve. The ATPase rate *versus* [M13 ssDNA] fit to a Equation 1 with a k_{cat} of 64.9 + 1.0 s^{-1} and a K_m of 0.63 + 0.04 nM. (B) 3 nM M13 ssDNA (●), 1.2 nM pGEX-5X-1 plasmid dsDNA (▼), or no DNA (○) was mixed with 100 nM SARS-CoV helicase, 2 mM ATP, 5 mM $MgCl_2$ in buffer A at 37 °C. After various times, the reactions were quenched by adding color-developing solution and released P_i was quantified using P_i standard curve. Steady state ATPase rate was obtained from the slope. ATPase rates were 54.2 s^{-1} (M13 ssDNA), 1.3 s^{-1} (pGEX-5X-1 plasmid dsDNA), and 0.9 s^{-1} (no DNA), respectively.

energy generated from NTP hydrolysis is necessary for efficient movement. It has been reported that DNA or RNA stimulates NTP hydrolysis 10- to 100- fold.[24-26] Interestingly, SARS-CoV helicase does not stimulate ATP hydrolysis activity in the presence of dsDNA, indicating that SARS-CoV helicase does bind only ssNA but not dsNA. Previous dsDNA unwinding experiment with fully dsDNA (blunt ended) did not show dsDNA unwinding activity, which supports our current results.[25] In general, the binding of ssNA stimulates the NTPase activity of helicases, which is believed that ssNA induces protein conformational change and allow the NTP hydrolysis to proceed.[27] Comparison of the kinetic parameters in the presence of poly(U) and M13 ssDNA suggests that SARS-CoV helicase does not show strict selectivity for ssNA, although k_{cat} value of poly(C) is lower than other ssNA. In contrast to SARS-CoV helicase classified as superfamily 1, hepatitis C virus (HCV) helicase, other RNA helicase that belongs to superfamily 2, binds a DNA substrate 40-times faster than RNA and shows better DNA unwinding activity than RNA.[28] Based on these results, ATPase activity experiments with SARS-CoV helicase were performed with M13 ssDNA hereafter.

The pH dependence of ATPase activity in the presence of M13 ssDNA shows that the optimal pH condition exists within the range of 6.2 to 6.6 (Fig. 3). On the contrary, steady state rates of ATPase activity below 6.0 and above 7.0 decreased less than 70% of maximum value. Previous studies have shown that nucleotide hydrolysis activity of helicase is greatly enhanced by binding to ssNA. Therefore, the factors that influence on the binding to NA, such as pH or metal ions, could be responsible for ATPase activity of SARS-CoV helicase. It is well known that the activities of enzymes are dependent on pH in the same way of acid-base ionization. In fact, many helicases show their optimum nucleotide hydrolysis activities at different pH conditions (for example, T7 bacteriophage helicase; pH 7.6,[29] Hepatitis C virus NS3h helicase; pH 7.0,[30] *E.coli* DnaB helicase; pH 8.1[31] *etc*). In the case of SARS-CoV helicase, the optimal pH for ATP hydrolysis is a little lower than other helicases.

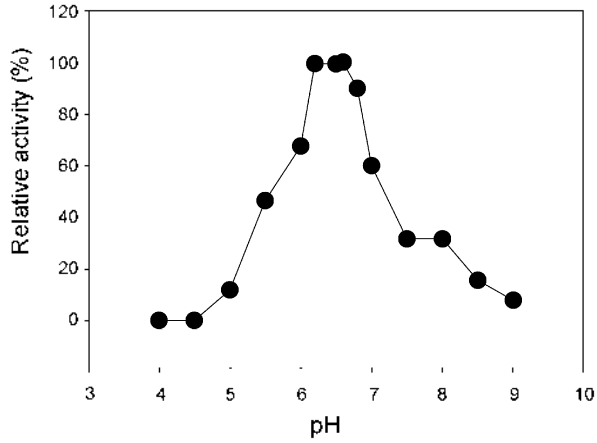

Figure 3. pH dependence profile of ATPase activity. ATPase rates were measured with 100 nM SARS-CoV helicase, 2 mM ATP, 5 mM $MgCl_2$, 2 nM M13 ssDNA, and 50 mM NaCl in several buffer solutions at 37 °C and at various pH. The ATPase activity was normalized to the maximal activity.

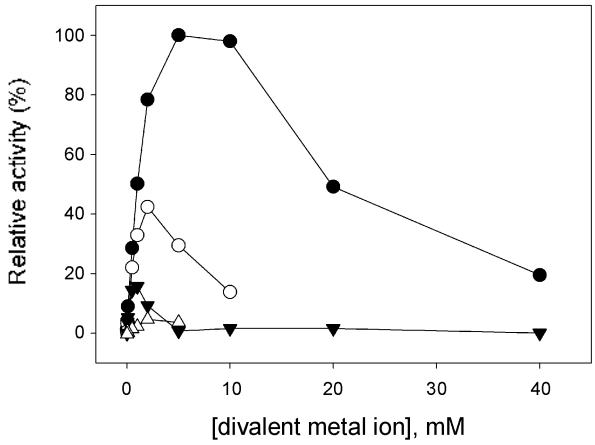

Figure 4. Dependence of ATPase rate on the concentration of various divalent metal ions. 100 nM helicase was mixed with 2 mM ATP, 2 nM M13 ssDNA, and various concentrations of $MgCl_2$ (●), $MnCl_2$ (○), $CaCl_2$ (△), and Zinc acetate (▼) in buffer A at 37 °C. The ATPase activity was normalized to the maximal activity obtained with $MgCl_2$.

In general, optimal pH conditions for dsNA unwinding and NTPase activity are similar unless salt concentrations change. Thus, it is expected that optimal pH conditions for dsNA unwinding would be similar to ATPase activity. Our results provide the basic experimental information for further studies of ATP hydrolysis and nucleic acid unwinding by SARS-CoV helicase.

Since there have been many reports regarding the stimulated NTPase activity by RNA virus helicases with divalent cations, the stimulatory effects of divalent metal ions on ATP hydrolysis by SARS-CoV helicase were investigated using four different kinds of metal ions. Steady state ATP hydrolysis experiments were carried out in the presence of Mg^{2+}, Mn^{2+}, Ca^{2+}, and Zn^{2+}. Fig. 4 shows the effect of divalent metal ion concentrations on the ATPase activity. Among the divalent cations tested, Mg^{2+} shows the optimal stimulation of ATPase activity. ATPase activity increases up to 5 mM of Mg^{2+}, and decrease thereafter. Mn^{2+} could be a substitute for Mg^{2+}, but the highest ATPase activity at 2 mM Mn^{2+} is only about 40% of Mg^{2+} at 5 mM. In the case of Ca^{2+} or Zn^{2+}, the maximum ATPase activity was less than 20% of Mg^{2+}. Recent computer-based three dimensional model of SARS-CoV helicase showed that it has six conserved motifs that are characteristic for superfamily 1 helicases, and motif I and II, specifically Lys288 residue in motif I by contacting the β-phosphate of the bound NTP, play an important role when NTP-Mg^{2+} complex binds the helicase and proceed to hydrolyze.[32] In addition, the complex ATP with SARS-CoV helicase closely resembles the crystal structure of PcrA helicase, another member of superfamily 1 helicases, which suggests that SARS-CoV helicase may follow similar divalent cation dependent ATP hydrolysis pattern of other superfamily 1 helicases. In previous studies of PcrA[33], Mg^{2+} binding can stabilize ATP-Mg^{2+} complex in the correct conformation to hydrolyze ATP. Likewise in the computer-based model of SARS-CoV helicase, Lys37 residue of PcrA is positioned at the Mg^{2+} binding site and is important for ATP hydrolysis through conformational change.

Here we report the studies of ATP hydrolysis activities by SARS-CoV helicase in the presence of various NAs, divalent cations, and at different pH. We demonstrate that ATPase activity is stimulated by ssNA and k_{cat}/K_m value is the highest in the presence of M13 ssDNA. ATP hydrolysis by the helicase is also influenced by pH conditions of reaction. As other superfamily 1 helicase, Mg^{2+} shows the optimal metal ion cofactor for ATP hydrolysis. Taken together, we provide basic analysis of ATPase activity and optimal ATPase reaction condition for further studies to develop the helicase-target antiviral inhibitors.

Acknowledgments. This work was supported by the Korea Research Foundation Grant funded by the Korean Government (MOEHRD) (KRF-2006-312-C00594) and Seoul R&BD program (10580) endowed to Y-J. J. and by a grant (2008040 1034026) from the BioGreen 21 Program, Rural Development Administration, Republic of Korea, endowed to D-E. K.

References

1. Patel, S. S.; Picha, K. M. *Annu. Rev. Biochem.* **2000**, *69*, 651.
2. Patel, S. S.; Donmez, I. *J. Biol. Chem.* **2006**, *281*, 18265.
3. Lohman, T. M.; Bjornson, K. P. *Annu. Rev. Biochem.* **1996**, *65*, 169.
4. Ellis, N. A.; Groden, J.; Ye, T. Z.; Straughen, J.; Lennon, D. J.; Ciocci, S.; Proytcheva, M.; German, J. *Cell* **1995**, *83*, 655.
5. Yu, C. E.; Oshima, J.; Fu, Y. H.; Wijsman, E. M.; Hisama, F.; Alisch, R.; Matthews, S.; Nakura, J.; Miki, T.; Ouais, S.; Martin, G. M.; Mulligan, J.; Schellenberg, G. D. *Science* **1996**, *272*, 258.
6. Gray, M. D.; Shen, J. C.; Kamath-Loeb, A. S.; Blank, A.; Sopher, B. L.; Martin, G. M.; Oshima, J.; Loeb, L. A. *Nature Genet.* **1997**, *17*, 100.
7. Marra, M. A.; Jones, S. J.; Astell, C. R.; Holt, R. A.; Brooks-Wilson, A.; Butterfield, Y. S.; Khattra, J.; Asano, J. K.; Barber, S. A.; Chan, S. Y.; Cloutier, A.; Coughlin, S. M.; Freeman, D.; Girn, N.; Griffith, O. L.; Leach, S. R.; Mayo, M.; McDonald, H.; Montgomery, S. B.; Pandoh, P. K.; Petrescu, A. S.; Robertson, A. G.; Schein, J. E.; Siddiqui, A.; Smailus, D. E.; Stott, J. M.; Yang, G. S.; Plummer, F.; Andonov, A.; Artsob, H.; Bastien, N.; Bernard, K.; Booth, T. F.; Bowness, D.; Czub, M.; Drebot, M.; Fernando, L.; Flick, R.; Garbutt, M.; Gray, M.; Grolla, A.; Jones, S.; Feldmann, H.; Meyers, A.; Kabani, A.; Li, Y.; Normand, S.; Stroher, U.; Tipples, G. A.; Tyler, S.; Vogrig, R.; Ward, D.; Watson, B.; Brunham, R. C.; Krajden, M.; Petric, M.; Skowronski, D. M.; Upton, C.; Roper, R. L. *Science* **2003**, *300*, 1399.
8. Rota, P. A.; Oberste, M. S.; Monroe, S. S.; Nix, W. A.; Campagnoli, R.; Icenogle, J. P.; Penaranda, S.; Bankamp, B.; Maher, K.; Chen, M. H.; Tong, S.; Tamin, A.; Lowe, L.; Frace, M.; DeRisi, J. L.; Chen, Q.; Wang, D.; Erdman, D. D.; Peret, T. C.; Burns, C.; Ksiazek, T. G.; Rollin, P. E.; Sanchez, A.; Liffick, S.; Holloway, B.; Limor, J.; McCaustland, K.; Olsen-Rasmussen, M.; Fouchier, R.; Gunther, S.; Osterhaus, A. D.; Drosten, C.; Pallansch, M. A.; Anderson, L. J.; Bellini, W. J. *Science* **2003**, *300*, 1394.
9. Ziebuhr, J. *Curr. Opin. Microbiol.* **2004**, *7*, 412.
10. Holmes, K. V. *J. Clin. Invest.* **2003**, *111*, 1605.
11. Anand, K.; Ziebuhr, J.; Wadhwani, P.; Mesters, J. R.; Hilgenfeld, R. *Science* **2003**, *300*, 1763.
12. Kwong, A. D.; Rao, B. G.; Jeang, K. T. *Nat. Rev. Drug. Discov.* **2005**, *4*, 845.
13. Yang, N.; Tanner, J. A.; Wang, Z.; Huang, J. D.; Zheng, B. J.; Zhu, N.; Sun, H. *Chem. Commun. (Camb)* **2007**, *42*, 4413.
14. Yang, N.; Tanner, J. A.; Zheng, B. J.; Watt, R. M.; He, M. L.; Lu, L. Y.; Jiang, J. Q.; Shum, K. T.; Lin, Y. P.; Wong, K. L.; Lin, M. C.; Kung, H. F.; Sun, H.; Huang, J. D. *Angew. Chem. Int. Ed.*

Engl. **2007**, *46*, 6464.
15. Tanner, J. A.; Zheng, B. J.; Zhou, J.; Watt, R. M.; Jiang, J. Q.; Wong, K. L.; Lin, Y. P.; Lu, L. Y.; He, M. L.; Kung, H. F.; Kesel, A. J.; Huang, J. D. *Chem. Biol.* **2005**, *12*, 303.
16. Lee, C.; Lee, J. M.; Lee, N. R.; Jin, B. S.; Jang, K. J.; Kim, D. E.; Jeong, Y. J.; Chong, Y. *Bioorg. Med. Chem. Lett.* **2009**, *19*, 1636.
17. Shum, K. T.; Tanner, J. A. *Chembiochem.* **2008**, *9*, 3037.
18. Jang, K. J.; Lee, N. R.; Yeo, W. S.; Jeong, Y. J.; Kim, D. E. *Biochem. Biophys. Res. Commun.* **2008**, *366*, 738.
19. Levin, M. K.; Patel, S. S. *J. Biol. Chem.* **2002**, *277*, 29377.
20. Jeong, Y. J.; Kim, D. E.; Patel, S. S. *J. Biol. Chem.* **2004**, *279*, 18370.
21. Sambrook, J.; Fritsch, E. F.; Maniatis, T. In *Molecular Cloning, A Laboratory Manual*, Second ed.; Ford, N.; Nolan, C.; Ferguson, M., Eds.; Cold Spring Harbor Laboratorty Press: 1989.
22. Piper, J. M.; Lovell, S. J. *Anal. Biochem.* **1981**, *117*, 70.
23. Tanner, J. A.; Watt, R. M.; Chai, Y. B.; Lu, L. Y.; Lin, M. C.; Peiris, J. S.; Poon, L. L.; Kung, H. F.; Huang, J. D. *J. Biol. Chem.* **2003**, *278*, 39578.
24. Washington, M. T.; Rosenberg, A. H.; Griffin, K.; Studier, F. W.; Patel, S. S. *J. Biol. Chem.* **1996**, *271*, 26825.
25. Patel, S. S.; Rosenberg, A. H.; Studier, F. W.; Johnson, K. A. *J. Biol. Chem.* **1992**, *267*, 15013.
26. Matson, S. W.; Richardson, C. C. *J. Biol. Chem.* **1983**, *258*, 14009.
27. Kadare G.; Haenni, A. L. *J. Virol.* **1997**, *71*, 2583.
28. Pang, P. S.; Jankowsky, E.; Planet, P. J.; Pyle, A. M. *EMBO J.* **2002**, *21*, 1168.
29. Jeong, Y. J.; Kim, D. E.; Patel, S. S. *J. Biol. Chem.* **2002**, *277*, 43778.
30. Levin, M. K.; Patel, S. S. *J. Biol. Chem.* **1999**, *274*, 31839.
31. Rajendran, S.; Jezewska, M. J.; Bujalowski, W. *J. Mol. Biol.* **2000**, *303*, 773.
32. Hoffmann, M.; Eitner, K.; von Grotthuss, M.; Rychlewski, L.; Banachowicz, E.; Grabarkiewicz, T.; Szkoda, T.; Kolinski, A. *J. Comput. Aided Mol. Des.* **2006**, *20*, 305.
33. Soultanas, P.; Dillingham, M. S.; Velankar, S. S.; Wigley, D. B. *J. Mol. Biol.* **1999**, *290*, 137.